

Time-delay Estimation in Time-warping Environments

Joshua N. Ash and Randolph L. Moses

Ohio State University, Dept. of Electrical and Computer Engineering, Columbus, Ohio, USA

ABSTRACT

Time-delay estimation (TDE) is a common requirement of the ranging and localization systems often found in unattended ground sensors. In this paper we consider novel approaches to the TDE problem in a time-warping acoustic environment, such as that encountered when the propagation velocity is not constant—due to wind gusts, for example. An increasing propagation velocity induces a compression of the received signal, while a diminishing velocity dilates the signal. These effects warp the shape of the received signal and can significantly reduce the effectiveness of traditional TDE algorithms

This paper presents algorithms and performance bounds for TDE in random velocity environments. We model unknown signal warping as a low-pass random process, which serves as a form of non-additive noise in the time-delay estimation problem. For warping environments, we propose computationally efficient non-parametric algorithms for TDE that significantly outperform traditional time-delay estimators, such as the location of the sample cross-correlation peak. The Cramér-Rao bound for TDE in a time-warping environment is also presented and used to evaluate the proposed estimators. Simulations demonstrate the bounds and estimator performance for acoustic signals.

Keywords: Time-delay estimation (TDE), time-difference of arrival (TDOA), signal warping, velocity profile, Cramer-Rao bound (CRB)

1. INTRODUCTION

Many ranging and localization systems rely on time-delay estimation (TDE) in order to determine the distance between a receiver and a distant source. If a signal $s(t)$ is transmitted by the source, the goal in TDE is to estimate the delay τ of the received signal $s(t - \tau)$. When the propagation velocity, c , is constant and known, the estimated delay may be used to compute the source-receiver distance as $c\tau$. This is known as time-of-arrival (TOA) ranging, and TDE is a critical component. TDE is also central to time-difference-of-arrival (TDOA) systems which require concurrent arrival time estimation at multiple receivers.^{1,2}

In practice a signal's propagation velocity is not constant, but rather varies slowly over distance and time due to environmental effects such as wind. Clearly, this becomes a problem when TDE is performed over large distances or when the signals have a large time extent—as is the case when lengthy signals are used to increase the energy of a transmitted calibration signal. If the propagation velocity is constant, and noise is additive, white, and Gaussian, then it is well-known that the maximum likelihood estimator for time-delay is given as the delay that maximizes the sample cross-correlation between the received signal and the transmitted signal [3, Ch. 7]. However, when the propagation velocity is not constant, this and other established techniques may have very poor performance.

An increasing propagation velocity means that subsequent samples of a transmitted signal will arrive slightly before they would have otherwise arrived if the velocity was not increasing. This induces a compression of the transmitted signal at the receiver. Conversely, if the propagation velocity is decreasing, subsequent samples will arrive slightly later than they would otherwise, effectively dilating the signal. These compressions and dilations impose a warping of the transmitted signal at the receiver which may be modeled as a time-varying delay, $\tau(t)$, on the received signal $s(t - \tau(t))$. The distorted signal shape which occurs in time-warping environments has a large negative impact on traditional TDE methods, such as cross-correlation.

Figure 1 illustrates this for a 40 s acoustic signal propagating a distance of 3 km with an average propagation velocity 343 m/s. Part (a) depicts a slowly varying (mostly decaying) velocity profile, as might be experienced

Corresponding author: J. Ash, E-mail: ashj@ece.osu.edu

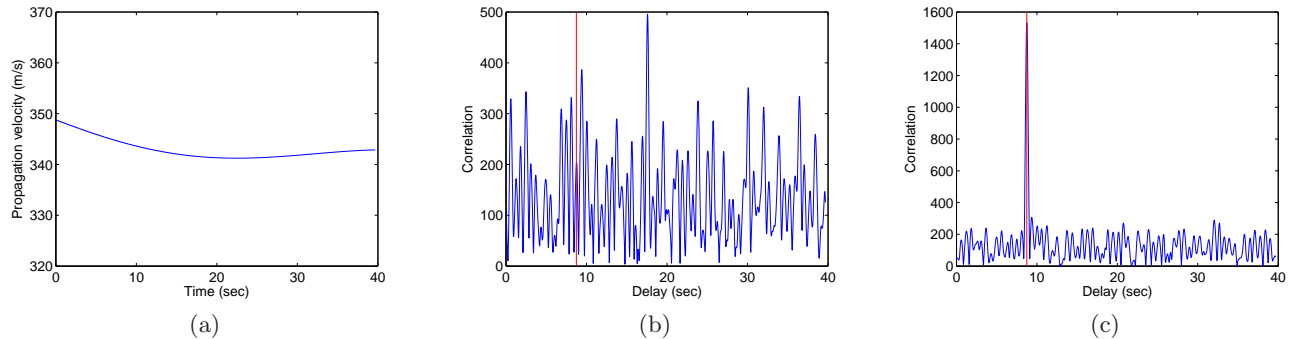


Figure 1. Non-constant propagation velocity example. (a) Sample time-varying propagation velocity profile for acoustics, and (b) resulting transmit-receive cross-correlation function. The cross-correlation is very irregular and peaks at a delay much greater than the true delay (vertical line). (c) Cross-correlation for constant propagation velocity.

from wind blowing from the receiver toward the source. The total velocity fluctuation is 7.5 m/s. Part (b) illustrates the transmit-receive cross-correlation using the time-warped reception from the velocity profile in (a). The signal and noise parameters of the example are further described in Section 2.2. In contrast, Part (c) illustrates the transmit-receive cross-correlation for the same signal and noise but with a constant propagation velocity of 343 m/s. In the constant velocity case, the correlation peak is well-defined and occurs at the true delay of $3000/343 \approx 8.7$ s (indicated by the vertical bar). The correlation function in the time-warped environment is severely degraded—with many local maxima—and the peak is offset over 8 s from the true delay.

In this paper we consider alternative TDE methods that are robust to signal warping. While the analysis and methods derived are general, the examples are drawn from long-duration acoustic signals with slowly varying propagation velocities. The remainder of the paper is organized as follows. In Section 2 we describe the signal model considered and present Cramér-Rao bounds indicating the best possible estimation performance in a time-warping environment. In Section 3 we present two non-parametric estimators based on pseudo-correlation functions that are robust to warping of the received signal. Finally, Section 4 provides conclusions and a summary of the estimators.

2. SIGNAL MODEL AND BOUNDS

We assume that the transmitted signal is described by a baseband signal $\tilde{g}(t)$ which is modulated onto a carrier with center frequency f_c . Thus, the transmitted passband signal is described as $s(t) = \text{Re}\{\tilde{g}(t)e^{j(w_c t + \phi_{tx})}\}$, where $w_c = 2\pi f_c$ and ϕ_{tx} is the carrier phase. For a delay τ , the received signal is

$$r_{pb}(t) = s(t - \tau(t)) + \xi(t) \quad (1)$$

$$= \text{Re}\{\tilde{g}(t - \tau(t))e^{jw_c(t - \tau(t))}e^{j\phi_{tx}}\} + \xi(t) \quad (2)$$

where $\xi(t)$ is passband noise, and we write the delay as $\tau(t)$ to emphasize the fact that it is time-varying. After mixing down to baseband, filtering out the double carrier component, and sampling at $t_n = n \Delta_t$, the sampled complex baseband signal may be written

$$r(t_n) = \underbrace{\tilde{g}(t_n - \tau(t_n))}_1 \underbrace{e^{-jw_c \tau(t_n)}}_2 e^{j\phi_{tx}} + \underbrace{e_n}_3. \quad (3)$$

The collection of samples $\{r(t_n)\}$, $n = 1 \dots N$ are used to estimate the delay elements τ . The noise e_n is assumed to be complex circular white Gaussian noise with variance σ_e^2 .

From (3), we see that the received baseband signal is *not* merely a time-warped version of the original baseband signal. Corresponding to the underbraces in (3), there are three types of distortion that complicate time-delay estimation: 1) The baseband signal $\tilde{g}(t)$ is not simply delayed by a constant amount, but rather has a

warped shape because the delay τ is time-varying. 2) The factor $e^{-jw_c\tau(t_n)}$ induces phase noise on the (already warped) baseband signal. While τ is expected to be a slowly varying random process, the multiplication by w_c can cause a slowly changing τ to induce rapid phase fluctuations. 3) Finally, additive noise is present, as in typical TDE problems.

In this paper we assume that the calibration signal $\tilde{g}(t)$ is a BPSK encoded pseudo-noise sequence. That is, for a random sequence of bits $b_i \in \{-1, 1\}$, $i = 1 \dots B$,

$$\tilde{g}(t) = e^{j\phi_0} \sum_{i=1}^B b_i p(t - iT_b), \quad (4)$$

where $p(t)$ is a given real-valued pulse shape that is only non-zero on $[0, T_b]$, and ϕ_0 is the phase offset of the binary symbols. Letting $g(t)$ equal the summation in (4) and $\tau_n = \tau(t_n)$, after substituting (4) into (3) the received baseband samples may be written

$$r(t_n) = g(t_n - \tau_n) e^{-jw_c\tau_n} e^{j\phi_{tx}} + e_n, \quad (5)$$

where ϕ_0 has been combined with the unknown carrier phase ϕ_{tx} and $g(t)$ is real-valued.

The transmit signal (4) has length $T_{max} = BT_b$ and is assumed to repeat indefinitely. Thus, (5) may be evaluated modulo T_{max} for values of $t_n > T_{max}$. Receivers record the time-warped reception and must determine the average delay of their reception from the start time of the signal. Clearly, delays greater than T_{max} cannot be distinguished from those in $[0, T_{max}]$.

2.1 Cramér-Rao Bound

In the most general setting, all of the delays $\{\tau_n\}$, $n = 1, \dots, N$ would have to be estimated. However, we assume that realizations of the random sequence $\{\tau_n\}$ exhibit significantly fewer degrees of freedom—as in the case of lowpass random processes—and model $\boldsymbol{\tau} = [\tau_1, \dots, \tau_N]^T$ as a linear combination of a small number of basis elements

$$\boldsymbol{\tau} = \boldsymbol{\Psi} \boldsymbol{x}, \quad (6)$$

where $\boldsymbol{\Psi} = [\boldsymbol{\psi}_1, \dots, \boldsymbol{\psi}_M]$ is an $N \times M$ matrix with orthogonal columns representing a basis set for potential warps, and $\boldsymbol{x} = [x_1, \dots, x_M]^T$ are parameters determining the realization of the warp. By convention we let $\boldsymbol{\psi}_1 = \mathbf{1}_N$, an N -vector of ones. Because all other basis vectors are assumed orthogonal to $\boldsymbol{\psi}_1$, this implies that x_1 represents the mean delay; or that $x_1 = \bar{\tau}$. Under this model, the parameter vector becomes $\boldsymbol{\theta} = [\phi_{tx}, x_1, \dots, x_M]^T$.

Substituting (6) into (5) and combining with the assumption of Gaussian noise e_n enables us to write the full probability density function (pdf) of the observations $\mathbf{r} = [r(t_1), \dots, r(t_N)]^T$ parameterized by $\boldsymbol{\theta}$, i.e. $p(\mathbf{r}; \boldsymbol{\theta})$. The Fisher information matrix (FIM) may then be computed as³

$$J_\theta = E \left[\left(\frac{\partial \ln p(\mathbf{r}; \boldsymbol{\theta})}{\partial \boldsymbol{\theta}} \right) \left(\frac{\partial \ln p(\mathbf{r}; \boldsymbol{\theta})}{\partial \boldsymbol{\theta}} \right)^T \right] \quad (7)$$

and used to calculate the Cramér-Rao bound (CRB). If $\hat{\tau}$ is any unbiased estimator of the mean delay $\bar{\tau} = x_1$, then the CRB asserts

$$\text{var}(\hat{\tau}) \geq [J_\theta^{-1}]_{2,2}, \quad (8)$$

because $\bar{\tau} = x_1$ is the second element of the parameter vector $\boldsymbol{\theta}$. In the examples below, $\boldsymbol{\Psi}$ is chosen to represent lowpass warps.

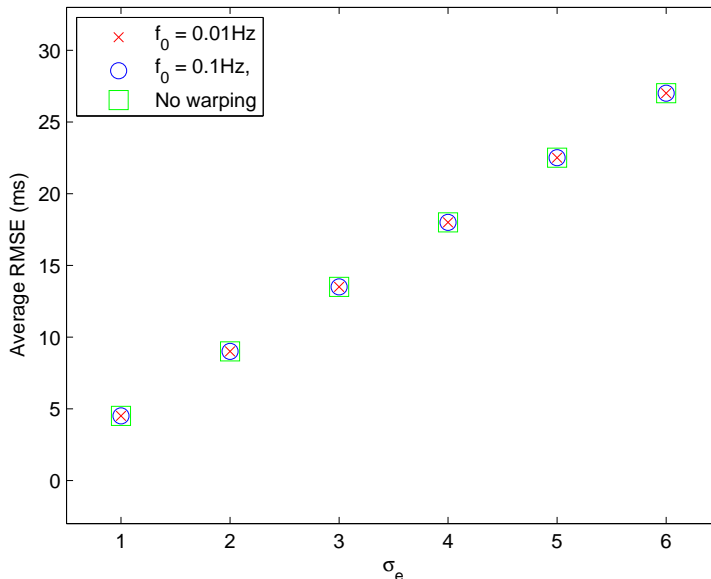


Figure 2. CRB-predicted time-delay estimation error in time warping and non-warping environments versus measurement noise standard deviation. The time warps are modeled as lowpass random process with cutoff frequencies $f_0 = 0.1$ Hz and 0.01 Hz. All three cases have nearly identical lower bounds.

2.2 Example

As an example, we consider a 40 s acoustic signal using Hanning pulses

$$p(t) = \begin{cases} \frac{1}{2}(1 - \cos(2\pi t/T_c)), & t \in [0, T_c] \\ 0, & \text{otherwise} \end{cases}, \quad (9)$$

and $B = 63$ bits drawn from a Kasami sequence [4, Ch. 13]. The symbol period is therefore $T_b = 40/63 \approx 0.63$ s. The carrier frequency is $f_c = 20$ Hz, and the baseband signal is sampled at the rate $f_s = 1/\Delta_t = 100$ Hz. In Figure 2 we plot the average root-mean-square error bound for $\bar{\tau}$ given as

$$E_{\theta}[e_{\bar{\tau}}] = E_{\theta} \left[\sqrt{[J_{\theta}^{-1}]_{2,2}} \right], \quad (10)$$

where the expectation is taken empirically over 100 realizations of the parameters ϕ_{tx}, τ . We consider realizations of τ from two different power spectra; each flat and low pass with cutoff frequency, f_0 . The cutoff frequencies tested were $f_0 = 0.01$ Hz, which is well approximated with $M = 6$ basis elements for the 40s signal, and $f_0 = 0.1$ Hz, which is approximated with $M = 21$ basis elements. The magnitude of the two power spectra were chosen such that the standard deviation of the resulting $\{\tau_n\}$ sequence was $\sigma_{\tau} = 50$ ms. As a point of reference, we note that for acoustics, a propagation velocity fluctuation of ± 6 m/s will induce an arrival time fluctuation of approximately ± 50 ms over a distance of 1 km. The velocity warp in Figure 1(a) was generated from a $\{f_0 = 0.01$ Hz, $\sigma_{\tau} = 50$ ms $\}$ warp, and the source signal used in Figs.1(b) and 1(c) was generated from (4) and (9).

In Figure 2 the average RMSE bound (10) is plotted versus the observation noise standard deviation σ_e . Bounds for an unwarped signal ($\Psi = \mathbf{1}_N$) and the two low-pass signals are considered. The somewhat unexpected result is that the estimation performance for estimating $\bar{\tau}$ is nearly identical for the different warping power spectra, and that they are indistinguishable from the non-warping case. Thus, from a CRB perspective, the *excess* error introduced by the low-pass warps considered is negligible compared to the error already present in a non-warping environment. Because the sample cross-correlator (SCC) is the maximum likelihood estimator (MLE) for non-warping environments, it is conceivable that it would perform well—although not optimally—in

an environment with minimal time warping. Experimental results, similar to Figure 1(b), illustrate that this is clearly not the case: the SCC performs extremely poorly in warping environments. However, the analysis in this section suggests that the warping itself does not significantly degrade the timing information in the measured data. Therefore, alternative time-delay estimation methods that are designed to be robust to signal warping may be able to achieve non-warping estimation performance—although operating in a time warping environment. This is the subject of the next section.

3. ROBUST TIME-DELAY ESTIMATORS

In this section we present two time-delay estimators designed for robustness to slowly varying time delays. The estimators are non-parametric and produce estimates quantized to the sampling period.

3.1 Subsequence Cross-correlation Estimator

Sample cross-correlations do not work well in time warping environments because the time-varying delay distorts the shape of the received signal and destroys its correlation with the transmitted signal. Because we assume that the underlying warp is a slowly varying function with time, the warp can be assumed approximately constant over short intervals. Therefore, if the received signal is partitioned into small enough intervals, referred to as subsequences, each subsequence will undergo relatively little warping and will correlate well with a portion of the transmitted signal \tilde{g} .

A received signal of length $N = KL$ is divided into K length- N sequences $r_1(n), \dots, r_K(n)$ whose only non-zero elements are a length- L subsequence of the received signal

$$r_k(n) = \begin{cases} r(n), & (k-1)L + 1 \leq n \leq kL \\ 0, & \text{otherwise} \end{cases}. \quad (11)$$

A similar approach of dividing up the received signal was proposed in⁵ to combat fading in a non-warping environment. We then perform circular cross-correlation (\otimes) of each subsequence against the transmitted signal

$$R_k(\tau) = r_k(n) \otimes \tilde{g}(n) \quad (12)$$

and incoherently average the results

$$R_{\text{SSCC}}(\tau) = \frac{1}{K} \sum_{k=1}^K |R_k(\tau)|. \quad (13)$$

The estimate of the delay is taken as the lag value which maximizes (13)

$$\hat{\tau}_{\text{SSCC}} = \arg \max_{\tau} R_{\text{SSCC}}(\tau) \quad (14)$$

and is referred to as the subsequence cross-correlation (SSCC) estimator.

Figure 3 plots $R_{\text{SSCC}}(\tau)$ using $K = 20$ for the same signal and measurement sequences used in generating the simple cross-correlation in Figure 1(b). Unlike the simple cross-correlation, the peak of the pseudo-correlation $R_{\text{SSCC}}(\tau)$ is clearly discernable and occurs close to the true delay.

Using the previously described signal model in Section 2.2, Figure 4 demonstrates the performance of the SSCC estimator in a non-warping environment as a function of the number of subsequences K and for several different levels of observation noise $\sigma_e \in \{1, 2, 4, 6\}$. These noise levels correspond to SNR levels of -7dB, -13dB, -19dB, and -23dB, respectively; where the SNR is defined as $\|\tilde{g}\|/\|e\|$ for signal sequence \tilde{g} and noise sequence e .

The empirical RMSE was computed from 500 realizations of the received signal vector with randomization over $\bar{\tau} \in [0, T_{\text{max}}]$ and the additive noise. Although there is no warping in this example, a number of important points are illustrated. First we see that the SSCC estimator nearly achieves the CRB for small values of K and

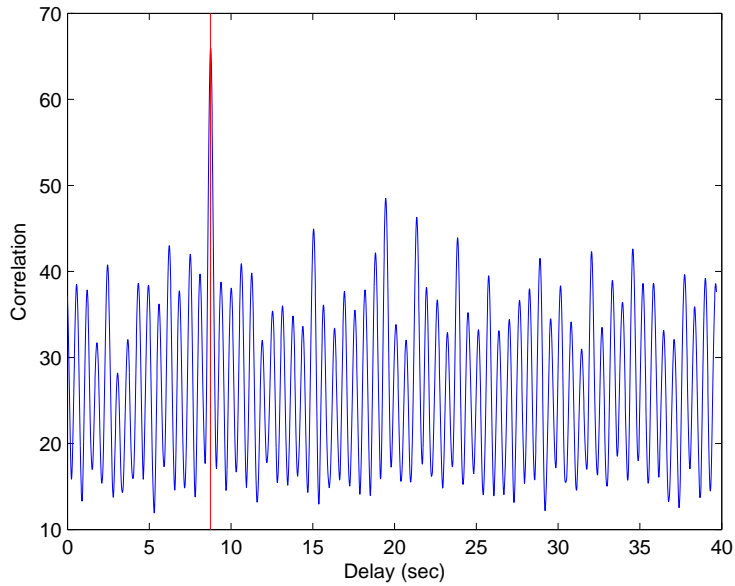


Figure 3. The composite correlation function $R_{SSCC}(\tau)$, using $K = 20$ subsequences, of the subsequence cross-correlation estimator applied to the example in Figure 1.

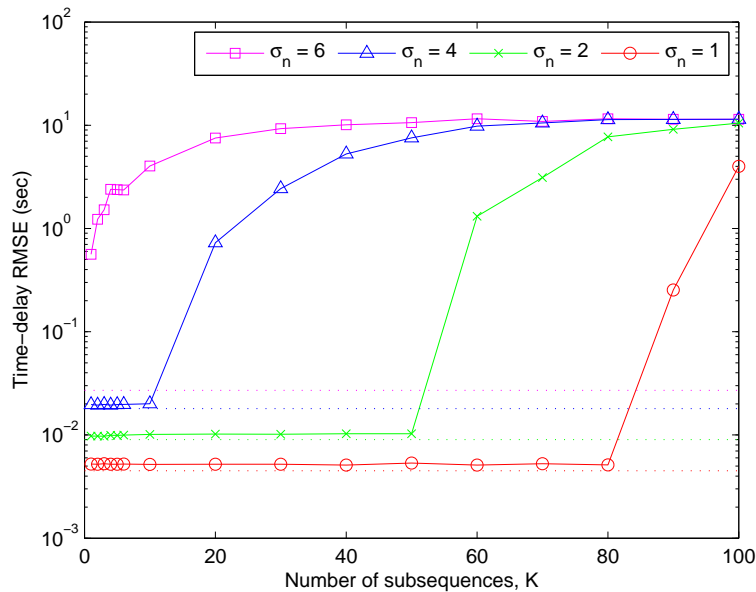


Figure 4. Performance of the subsequence cross-correlation estimator (SSCC) under constant warps; horizontal lines, from top to bottom, indicate CRBs for $\sigma_e = 6$ to $\sigma_e = 1$, respectively.

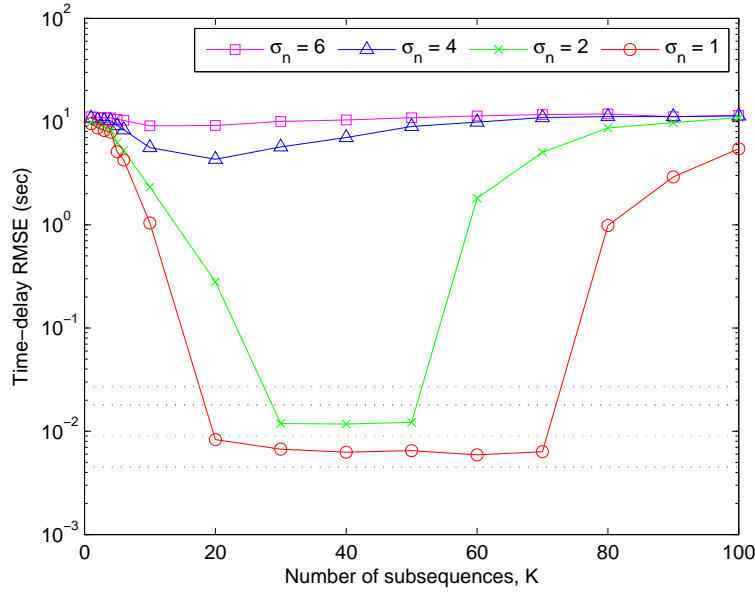


Figure 5. Performance of the subsequence cross-correlation estimator (SSCC) in a time-warping environment ($f_0 = 0.01$ Hz $\sigma_\tau = 50$ ms); horizontal lines, from top to bottom, indicate CRBs for $\sigma_e = 6$ to $\sigma_e = 1$, respectively.

σ_e . This is not surprising because a full-sequence cross-correlation ($K = 1$) is well-known to be the maximum-likelihood estimator (MLE) for this (constant delay) problem [3, Ch. 7]. The small offset for $\sigma_e = 1$ arises from quantization error due to the sampling rate of 100 Hz. When the noise is large, as in the $\sigma_e = 6$ case, the CRB is not achievable, even by the MLE. This is due to the well-known threshold effect in time-delay estimation.⁶ Second, for each noise level, there is a number of subsequences, which we will call K_{pg} , beyond which the RMSE rapidly increases. This is due to the loss in coherent processing gain that is incurred when the signal is divided into too many subsequences. When the noise level is large, greater processing gain is needed to push the effective SNR above the threshold required for CRB-level performance. Consequently, as the noise grows larger, the maximum number of subsequences that can be used to combat warping decreases.

Because the maximum estimable delay is T_{max} , the worst possible unbiased estimator chooses estimates uniformly among $[0, T_{max}]$. The standard deviation of a uniform random variable $U(0, T_{max})$ is $T_{max}/\sqrt{12}$, making the worst possible standard error in our example $40/\sqrt{12} \approx 11.5$ s. This is the maximum error seen in Figure 4.

Figure 5 demonstrates the performance of the SSCC estimator in the low-pass warping environment described above ($f_0 = 0.01$ Hz, $\sigma_\tau = 50$ ms); except for the warping, all other parameters remain the same as in Figure 4. Now, unlike the non-warping case, a single cross-correlation ($K = 1$) performs very poorly. As the number of subsequences is increased, we see improved performance as expected. In the $\sigma_e = 1$ and $\sigma_e = 2$ cases, the error is reduced nearly three orders of magnitude for some values of K and nearly obtains the CRB. As the noise grows larger, we observe that a larger number of subsequences are needed to combat the signal warping; we will call this minimum number of subsequences K_w . For $\sigma_e = 1$ we have $K_w \approx 20$ and for $\sigma_e = 2$, $K_w \approx 30$. As the noise level increases, K_w increases and K_{pg} decreases. As long as $K_w < K_{pg}$, there is a region that supports low estimation error; as seen for $\sigma_e = 1, 2$. If the noise is too great, the minimum number of subsequences needed to combat warping (K_w) is larger than the maximum number of subsequences needed for sufficient processing gain (K_{pg}) and large estimation error results; as seen for $\sigma_e = 4, 6$. In practice, K can be selected based on known signal and noise parameters, or it can be selected adaptively based on a set of quality metrics defined for the composite correlation function $R_{SSCC}(\tau)$; although, we do not explore these ideas in this paper.

3.2 Subsequence Range-Doppler Estimator

The SSCC method above is effective in overcoming time-warped signals, however in the presence of large noise the number of subsequences needed is large. This problem would be exaggerated if the warp function varied more rapidly. To improve this situation, we allow a more general form for the delay profile in each windowed subsequence while maintaining reasonable computational complexity. In this subsection we specifically consider linear warp profiles $\tau_k(t) = a_k t + b_k$ within each windowed subsequence k . Making this substitution, for each subsequence k , into Eq. (3) we obtain

$$r_k(t_n) = g(t_n - a_k t_n - b_k) e^{j(\phi_{tx} - w_c a_k t_n - w_c b_k)} \quad (15)$$

$$\approx g(t_n - b_k) e^{j\phi_k} e^{-jw_{d_k} t_n} \quad (16)$$

for time samples $\{t_n\}$ satisfying $(k-1)L + 1 \leq n \leq kL$. In forming the approximation (16), we make use of the assumption that the true delay τ is slowly varying and therefore $a_k \ll 1$. The phase terms are rewritten as a time-independent portion $\phi_k = \phi_{tx} - w_c b_k$ and a time-dependent portion $w_{d_k} = w_c a_k$. For each subsequence k , the measurement equation (16) has a range-Doppler interpretation where the unknown b_k is a range-induced time delay, ϕ_k is an unknown phase, and w_{d_k} is a Doppler frequency. In order to find the mean time delay, we form pseudo-correlations for each subsequence

$$R_k(b_k) = \arg \max_{w_{d_k}} |(r_k(n) e^{+jw_{d_k} t_n}) \otimes \tilde{g}(n)|. \quad (17)$$

The circular cross-correlation may be implemented using DFTs where $\mathcal{F}\{r_k(n) e^{+jw_{d_k} t_n}\}$ is efficiently computed from circular shifts of $\mathcal{F}\{r_k(n)\}$. Further, if some information is known about the range of a_k , then the search space for w_{d_k} may be appropriately reduced. As in the SSCC estimator, the time delay estimate is taken as the delay which maximizes the incoherent average of the per-sequence pseudo-correlations

$$\hat{\tau}_{\text{SSRD}} = \arg \max_b \frac{1}{K} \sum_{k=1}^K R_k(b). \quad (18)$$

We refer to this estimator as the subsequence range-Doppler (SSRD) estimator for time-delay estimation.

In Figure 6 we demonstrate the performance of the SSRD approach in a warping environment with signal and warping parameters as in the previous examples. Looking at the $\sigma_e = 1, 2$ cases, we see that the SSRD estimator achieves CRB-level performance with a much smaller number of subsequences when compared to the SSCC estimator. However, the high noise cases $\sigma_e = 4, 6$ remain unimproved.

4. CONCLUSIONS

Traditional methods of time-delay estimation were not designed to accommodate signals with time-varying delays—as encountered when the signal propagation velocity is not constant—and therefore exhibit very poor performance in these regimes. Using a linear basis representation for time-varying delays allowed us to parameterize viable signal warps and derive the Cramér-Rao bound for estimating the mean delay of a complex baseband signal in a time-warping environment. We demonstrated, for the lowpass warps considered, that the lower bound on TDE error remains essentially the same as in the unwrapped case. This motivated the search for novel TDE algorithms that were robust to signal warping.

The subsequence cross-correlation (SSCC) and subsequence range-Doppler (SSRD) estimators were developed on the principal that short subsequences of the received signal will undergo less warping than signal as a whole. These methods apply coherent processing within each subsequence and use incoherent combining across subsequences. The SSCC method assumes that the variable delay is approximately constant over subsequences, while the SSRD method make a piecewise linear assumption. These ideas may be extended to piecewise polynomials in order to model more complicated warping functions, however the fitting process becomes more complicated and prone to local convergence problems. The SSCC and SSRD algorithms afford numerically efficient implementations using discrete Fourier transform properties and do not require numerical optimization procedures.

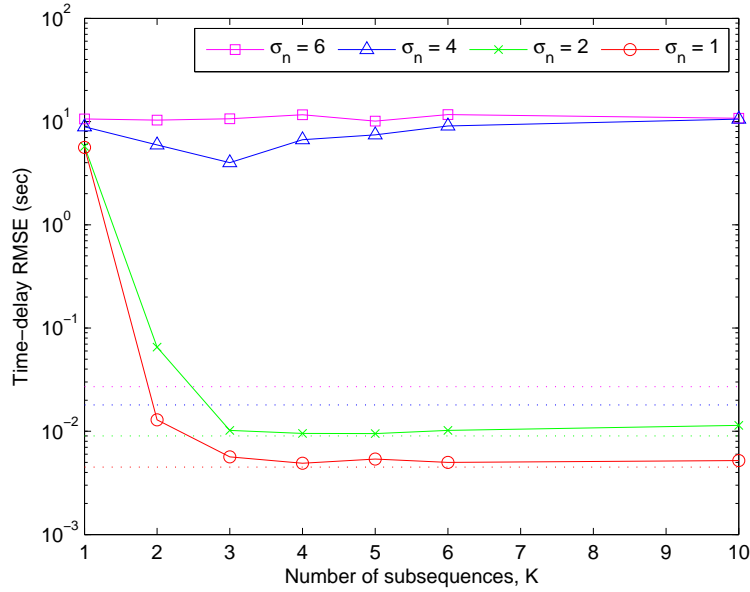


Figure 6. Performance of the subsequence range-Doppler (SSRD) estimator in a time-warping environment ($f_0 = 0.01$ Hz $\sigma_\tau = 50$ ms); horizontal lines, from top to bottom, indicate CRBs for $\sigma_e = 6$ to $\sigma_e = 1$, respectively.

Examples demonstrated that both methods performed significantly better than standard cross-correlation and that the proposed methods were effective in mitigating the negative effects of signal warping while performing time-delay estimation. For SNR values as low as -13dB, the proposed methods demonstrated CRB-level performance for the class of warping functions considered.

REFERENCES

- [1] Patwari, N., Ash, J. N., Kyperountas, S., Hero III, A. O., Moses, R. L., and Correal, N. S., "Locating the nodes: cooperative localization in wireless sensor networks," *IEEE Signal Processing Magazine* **22**, 54–69 (July 2005).
- [2] Gustafsson, F. and Gunnarsson, F., "Mobile positioning using wireless networks: possibilities and fundamental limitations based on available wireless network measurements," *IEEE Signal Processing Magazine* **22**, 41–53 (July 2005).
- [3] Kay, S. M., [*Fundamentals of Statistical Signal Processing, Volume I: Estimation Theory*], vol. 1, Prentice Hall (1993).
- [4] Proakis, J., [*Digital Communications*], McGraw-Hill, Boston, MA (1995).
- [5] Yousef, N., Sayed, A., and Jalloul, L., "Robust wireless location over fading channels," *IEEE Trans. Veh. Tech.* **52**, 117–126 (2003).
- [6] Weiss, A. J. and Weinstein, E., "Fundamental limitations in passive time delay estimation, Part I: Narrow-band systems," *IEEE Transactions on Acoustics, Speech, and Signal-Processing* **31**(2), 472–485 (April 1983).